*Journal of the Korean Nuclear Society*
*Volume 21, Number 2, June, 1989*

# Dynamic Strain Aging of Zircaloy-4 PWR Fuel Cladding in Biaxial Stress State

**Ki Seong Park and Byong-Whi Lee**
Korea Advanced Institute of Science and Technology
(Received February 17, 1989)

# 가압경수로용 지르칼로이-4 피복관의 2축 응력 인장시 동적 변형 시효

박기성 · 이병휘
한국과학기술원
(1989. 2. 17 접수)

## Abstract

The expanding copper mandrel test performed at three strain rates (3.2×10E−5 /s, 2.0×10E−6 /s and 1.2×10E−7 /s) over 553–873 K temperature range by varying the heating rates (8−10℃ / s, 1−2℃ / s and 0.5℃ / s) in air and in vacuum (5×10E−5 torr). The yield stress peak, the strain rate sensitivity minimum and the activation volume peaks could be explained in terms of the dynamic strain aging. The activation energy for dynamic strain aging obtained from the yield stress peak temperature and strain rate was 196 KJ/mol and this value was in good agreement with the activation energy for oxygen diffusion in α−zirconium and Zircaloy−2 (207−220 KJ/mol). Therefore, oxygen atoms are responsible for the dynamic strain aging which appeared between 573 K and 673 K. The yield stress increase due to the oxidation was obtained by comparing the yield stress in air with that in vacuum and represented by the percentage increase of yield stress ($\sigma_{y}$ − $\sigma_{y}$ / $\sigma_{y}$). The slower the strain rate, the greater the percentage increase occurs. In order to estimate the yield stress of PWR fuel cladding material under the service environment, the yield stress in water was obtained by comparing the oxidation rate in air that in water assuming the relationship between the oxygen pick-up amount and the yield stress increase.

## 요 약

지르칼로이−4 피복관에 대해서 3가지 변형 속도로(1.2×10E−7 / s, 2.0×10E−6 / s, 3.2×10E−5 / s), 553−873K의 온도 구간에서 구리 맨드렐 팽창 시험법을 공기와 진공(5×10E−5 torr) 분위기에서 수행했고, 변형 속도의 변화는 시편의 가열 속도를 조절함으로써 얻을 수 있었다. 각각의 변형 속도에서 항복 응력 피크와 변형 속도 감도 최저값 그리고 활성화 부피 극대값이 나타나는 이유는 동적변형시효 현상 때문이라고 설명된다. 항복 응력 피크가 나타나는 온도와 변형속도로부터 얻어진 동적변형시효의 활성화 에너지는 196(KJ / mol) 이었고 이 값은 α−지르코니움과 지르칼로이−2에서 활성화 에너지(207−220 KJ / mol)값

과 잘 일치한다. 그러므로 573−673K의 온도 구간에서 나타나는 동적변형시효 현상은 산소 원자 때문이라고 생각된다. 산화에 의한 항복 응력의 증가는 공기중 실험과 진공 실험으로 얻어진 항복 응력값을 비교함으로서 얻었고, 그것은 항복 응력의 증가 분율로 표시했다. 결과는 변형속도가 느릴 수록 증가 분율은 더욱 더 커짐을 알 수 있었다. 그리고 산소 침투량과 항복 응력 증가 사이의 관계가 직선적이라는 가정하에 공기와 수중에서의 산화 속도를 비교하여 수중에서의 항복 응력 값을 계산해 보았다.

## Nomenclature

$d$ : Initial clearance between mandrel outer radius and zircaloy inner radius at room temperature
$m$ : Strain rate sensitivity
$M$ : Taylor's factor
$Q$ : Activation energy for dynamic strain aging
$V_{app}$ : Apparent activation volume
$R$ : Gas constant : 8.314(J/mol K)
$k$ : Boltzmann's constant ; $1.38054\times10^{-23}(J/K)$
$k_p$ : Oxidation rate constant
$\Delta w_a$ : Weight gain in air test during test time
$\Delta w_w$ : Weight gain in water test during test time
$\Delta w_v$ : Weight gain in vacuum test during test time
$\delta w^a$ : $\Delta w_a - \Delta w_v$
$\delta w^w$ : $\Delta w_w - \Delta w_v$
$P_i$ : Percentage increase of the yield stress by comparing $\sigma_y{}^a$ with $\sigma_y{}^v$
$\sigma_y{}^a$ : Yield stress in air test
$\sigma_y{}^v$ : Yield stress in vacuum test
$\sigma_y{}^w$ : The predicted yield stress in water test
$\Delta\sigma_y{}^a$ : $\sigma_y{}^a - \sigma_y{}^v$
$\Delta\sigma_y{}^w$ : $\sigma_y{}^w - \sigma_y{}^v$
$\tau$ : Shear stress

## 1. Introduction

The high corrosion resistance and low neutron absorption characteristics of zirconium make it an ideal material for thermal nuclear reactor applications such as fuel cladding and pressure tube. Because of the highly reactive nature of zirconium, it is very diffcult to purify, and contains both substitutional and interstitial impurities. The interstitial impurities, O and N, have a profound effect on the strength of zirconium alloys and, at higher temperatures, oxygen has been shown to be largely responsible for the strain aging behaviour.

Strain aging is a well known phenomenon that occur in many materials. When a specimen is deformed beyond the yield point, unloaded, and then reloaded, sharp yield drop is not observed. However, if the specimen is aged sufficiently in the unloaded condition and test again, the yield point returns. At those temperatures where it is normally studied, this phenomenon usually occurs over a finite period of time. However, strain aging can be explained in terms of dislocation pinning by diffusing impurity atoms so that the kinetics of the process should depend largely on the diffusion rates of the impurity atoms. As a result strain aging phenomena may occur simultaneously with deformation if the temperature is suitably raised. When this happens, metal is said to undergo dynamic strain aging. The dynamic aspects of strain aging that have been identified are

(1) the discontinuous plastic *flow*[1,2,3,4,5],
(2) the appearance of plateaus or *peaks*[2,3,6,7] in the flow stress-temperature diagram,
(3) activation volume *peak*[8],
(4) low strain rate *sensitivity*[2,3,9]

Many of these phenomena have been related to some form of dynamic strain aging, and a variety of mechanisms have been proposed. However, these phenomena have not yet been adequately characterized because of the multiplicity of alloying elements and impurities.

Strain aging effect causes changes in ductility, yield point, hardness, and tensile strength. Especially, ductility reduction is important because it induces the brittle fracture of clad. The present test temperature range is 553 to 873 K, and this intermediate temperature range covers not only the range of the Zircaloy–4 normal operating and abnormal transient condition in PWR, but also the range inducing strain aging effect of Zircaloy–4. Therefore, dynamic strain aging was investigated in order to assess the potential effect on PWR fuel clad brittle fracture particularly in the ramping and load following cycle.

And the oxidation also induces ductility reduction. The strength properties increase and the ductility decreases as the oxygen content increases. This strengthening is due to the oxygen diffusion into the materials and the stable oxide layer formation.

The purpose of this study is

(1) to identify strain aging behavior by obtaining temperature sensitive yield pressure, yield stress, strain rate sensitivity, and apparent activation volume.

(2) to identify the solute responsible for dynamic strain aging by obtaining activation energy for dynamic strain aging from a shift of the yield stress peak temperature with the change in strain rate. The activation energy for dynamic strain aging is equal to that of solute diffusion responsible for dynamic strain aging.

(3) to obtain the oxidation effect on mechanical properties of Zircaloy-4 by comparing yield stress obtained in air with that in vacuum [$5-10^{-5}$ torr] and the quantitative oxidation effect of the water environment by comparing relative oxidation rate in air with that in water assuming the linear relationship between the oxygen pick-up amount and the yield stress increase.

## 2. Theory

### 2.1 Yield Pressure and Yield Stress of Zircaloy Tube

The yield *pressure*[10] is actually equal to the equilibrium pressure. This assumption is reasonable since the zircaloy tube used in mandrel test experiences a little plastic deformation. Under the present experimental condition, the stress state is biaxial ($\sigma_z=0$), and other widely used test is uniaxial tensile test. Therefore, to compare the present experimental results, converting the biaxial condition to uniaxial condition is necessary. For this, yield pressure is converted to yield stress by maximum shear strain energy theory (Von-Mises' yield *criterion*[11,12]).

### 2.2 Dynamic Strain Aging

#### 2.2.1 Characteristics of Dynamic Strain Aging

In zirconium alloys, the yield stress peak which is a manifestation of dynamic strain aging appears in the yield stress versus temperature diagram. In general, this peak due to dynamic strain aging has its maximum potential at some intermediate temperature. At low temperatures, the mobility of solute atoms is so low that they effectively cannot keep up with the moving dislocations and, at higher temperatures, the mobility of solutes is so high that they can easily move with the dislocations and again cannot exert strong drag force. From these consideration, we can also deduce that this peak is strain rate and temperature dependent. Namely, when the strain rate rises, a peak moves towards high temperature.

#### 2.2.2 Activation Energy for Dynamic Strain Aging

From the above considerations, we can conclude that the activation energy obtained from a shift of the yield stess peak temperature with the change in strain rate is equal to that of dynamic strain aging and in turn to that of solute diffusion.

A ctivation *energy*[13] for dynamic strain aging is obtained as follows,

$$\dot{\varepsilon} = A \exp\left(\frac{-Q}{RT}\right) \quad \cdots\cdots (1)$$

By taking logarithms on both sides of Eq. (1):

$$\ln \dot{\varepsilon} = \ln A + \left(\frac{-Q}{RT}\right) \quad \cdots\cdots (2)$$

where Q is the activation energy for dynamic strain aging, T is the yield stress peak temperature, A is the material constant and R is the gas constant (8.314 Joule/mole K). By plotting the $\ln \dot{\varepsilon}$ versus 1/T, we can obtain a straight line, and it is evident that

$$slope = \frac{-Q}{R} \quad \cdots\cdots (3)$$

therefore, activation energy for dynamic strain aging, Q, is given by:

$$Q = -R \times slope \quad \cdots\cdots (4)$$

### 2-2-3 Strain Rate Sensitivity

The strain rate *sensitivity*[11], m, is the increase in stress needed to cause a certain increase in plastic strain rate at a given level of plastic strain and a given temperature. This value can be obtained by following equations.

$$m = \left(\frac{\partial \ln \sigma}{\partial \ln \dot{\varepsilon}}\right)_{\varepsilon, T} = \frac{\ln(\sigma_2 / \sigma_1)}{\ln(\dot{\varepsilon}_2 / \dot{\varepsilon}_1)} \quad \cdots\cdots (5)$$

In general, the strain rate sensitivity tends to increase more or less linearly with temperature in a number of metals. When it falls below this straight line dynamic strain aging phenomena are also observed.

### 2-2-4 Apparent Activation Volume

The apparent activation volume associated with the deformation process has been obtained from the following classical *equations*[14,15],

$$V_{app} = kT \frac{\partial \ln \dot{\varepsilon}}{\partial \tau} = kT \frac{\ln(\dot{\varepsilon}_1 / \dot{\varepsilon}_2)}{\tau_1 - \tau_2} \quad \cdots\cdots (6)$$

where k is a Boltzmann's constant, $\dot{\varepsilon}$ is the strain rate, $\tau_1$ and $\tau_2$ are the applied shear stresses at the normal strain rates $\dot{\varepsilon}_1$ and $\dot{\varepsilon}_2$ and T is the absolute temperature. The shear stress $\tau$ was calculated from the yield stress $\sigma_y$, using the following relation,

$$\tau = \sigma_y / M \quad \cdots\cdots (7)$$

where M is the Taylor factor. According to Luton et *al.*[16], M is assumed to be equal to 4. The peak in activation volume was explained in terms of dynamic strain aging.

## 3. Experiment

### 3.1 Mandrel Test

Generally, cladding failures occur during steep power increase. That is, as the power increase rapidly, the different thermal expansion coefficient between uranium-dioxide and zircaloy cladding cause contact between them in biaxial stress state. If internal pressure which is induced by contact is greater than yield stress of zircaloy cladding, the clad deform plastically.

This experiment used copper as expanding mandrel which has about 2.6 times greater thermal expansion coefficient than Zircaloy-4 clad. This large value of thermal expansion coefficient difference is sufficient to simulate contact pressure between pellet and clad in biaxial stress state. But, the copper mandrel test has two limitations to its applications. First, the temperature limitation, that is, the temperature below 553 K is not applicable because induced plastic deformation of Zircaloy-4 cladding tube is too small to detect. Secondly, the strain-rate limitation, that is, the strain-rate above $10^{-5}$ $s^{-1}$ is not applicable because the heating rate above 10 ℃ / s is difficult in the experiments. The relation between heating-rate and strain-rate is as shown in fig.2 ; 10–8 ℃/s becomes to $3.2 \times 10^{-5}$s $^{-1}$, 1–2 ℃ / s becomes to $2.0 \times 10^{-6} s^{-1}$, and 0.5℃ / s becomes to $1.2 \times 10^{-7} s^{-1}$. These two limitations can be varied with sample size(tube and mandrel).

### 3.2 Materials

Stress-Relieved Zircaloy-4 PWR fuel cladding tube supplied by Sandvik, Sweden. Test specimens were cut in 25 mm length and its measured

dimensions are 9.487 mm inner diameter, 10.744 mm outer diameter and 0.629 mm wall thickness in average.

Copper mandrel is commercially provided 99% copper rod and it was machined 40 mm length and various diameter size to 0.005 mm accuracy to give various initial clearance, d, value.

### 3.3 Test Apparatus

The specimen set and the test apparatus are as shown in Fig 1. The specimen set is composed with copper mandrel, Zircaloy-4 tube and temperature measurement equipment. Temperature of specimen is measured with chromel-alumel medium size thermocouple. To reduce the initial copper mandrel diameter, liquid nitrogen is used. Therefore, copper mandrel is easily inserted into zircaloy tube. The induction furnace and supporter are used for heating the specimen uniformly. Rotary and diffusion pump are used for controlling the vacuum enviornment. The inner diameter of tube was measured with cylinder gauge and the outer diameter was measured with micrometer.

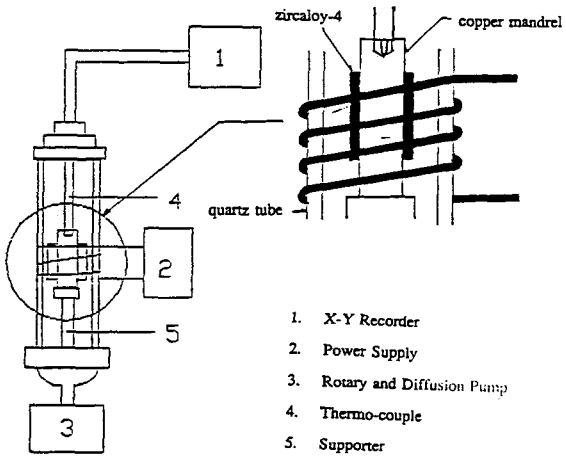


**Fig.1 Test Apparatus**

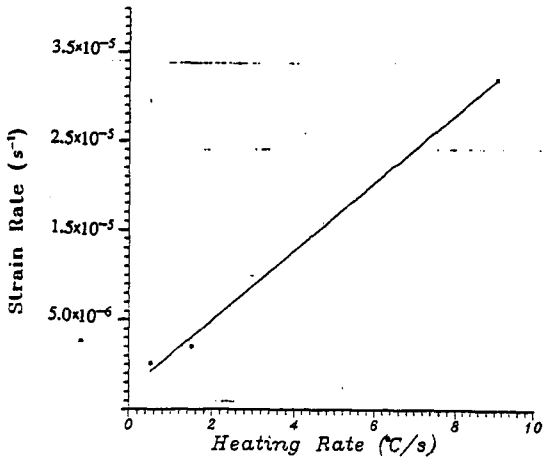


**Fig.2 Heating Rate vs. Strain Rate**

### 3.4 Procedure

The experimental procedures are as follows:

(1) Copper mandrel is inserted into zircaloy tube.
(2) Copper, zircaloy tube and temperature measurement system are assembled.
(3) Assembled specimen set is put into quartz tube.
(4) Test is accomplished in air or vacuum [$5\times10^{-5}$ torr] and power is controlled to give constant test temperature.
(5) Test temperature are 553, 598, 623, 648, 673, 698, 723, 748, 773, 823 and 873 K.
(6) If the temperature is reached to test temperature, after holding temperature for 3 minutes specimen set was cooled.
(7) After the specimen assembly temperature is cooled to room temperature, the inner and outer diameter changes are measured.

## 4. Results and Discussion

Experiments were conducted over temperature range of 553–673 K at $\dot{\varepsilon}=1.2\times10^{-7}s$, 573–798 K at $\dot{\varepsilon}=2.0\times10^{-6}s^{-1}$ and 473–823 K at $\dot{\varepsilon}=3.2\times10^{-5}s^{-1}$. After yield pressure was calculated from

this experimental results, yield stress, strain-rate sensitivity, activation volume and percentage increase of yield stress due to oxidation were obtained.

### 4.1 Yield Stress Versus Temperature

From the experimental results, the yield *pressures*[10] were calculated and are as shown in Fig.3, and the yield stress versus temperature is as shown in Fig 4. The trends of yield pressure and stress versus temperature were the same. The yield stress behavior from the present investigation is in close agreement with Derep et *al.*[7], *Grade*[17], Thorpe et *al.*[18], Ramachandran et al.[2] and Sherby et al.[9] Especially considering the strain rate, the present results are in good agreement with Ramachandran et *al.*[2] and *Grade*[17].

The yield stress peak temperature is a function of strain rate. From this experiments, the yield stress peak temperatures were 576 K at $\dot{\epsilon}=1.2\times 10^{-7}s^{-1}$, 623 K & 723 K at $\dot{\epsilon}=2.0\times10^{-6}s^{-1}$ and 673 K and 798 K at $\dot{\epsilon}=3.2\times10^{-5}s^{-1}$ in air and these peaks in vacuum were 576 K at $\dot{\epsilon}=1.2\times 10^{-7}s^{-1}$, 623 K at $\dot{\epsilon}=2.0\times10^{-6}s^{-1}$, 673 K at $\dot{\epsilon}=3.2\times10^{-5}s^{-1}$ These results correspond to 693 K ( $\dot{\epsilon}=3.3\times10^{-5}s^{-1}$, Zircaloy-4) by Derep et *al.*[7], 690 K ( $\dot{\epsilon}=1.33\times10^{-4}s^{-1}$, Zircaloy-4) by Hong et *al.*[19], 650 K ( $\dot{\epsilon}=1.33\times10^{-4}s^{-1}$, Zr-Nb) by Thorpe et *al.*[18], 598 K ( $\dot{\epsilon}=9.8\times10^{-4}s^{-1}$, Zircaloy-4) by Rheem et *al.*[20] and 573 K ( $\dot{\epsilon}=1.0\times10^{-3}s^{-1}$, Zr) by Ramachandran et *al.*[2].

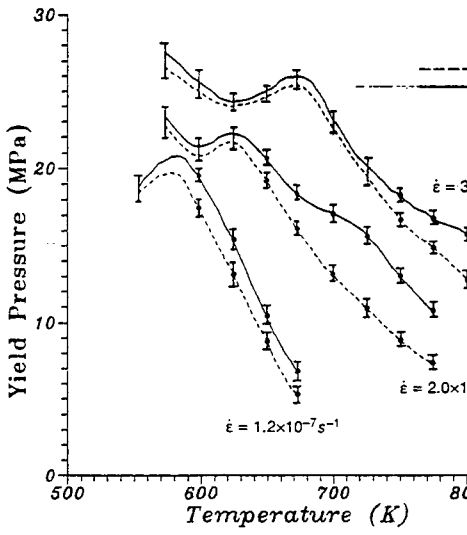


**Fig.3 Yield Pressure of Zircaloy-4 vs. Temperature**

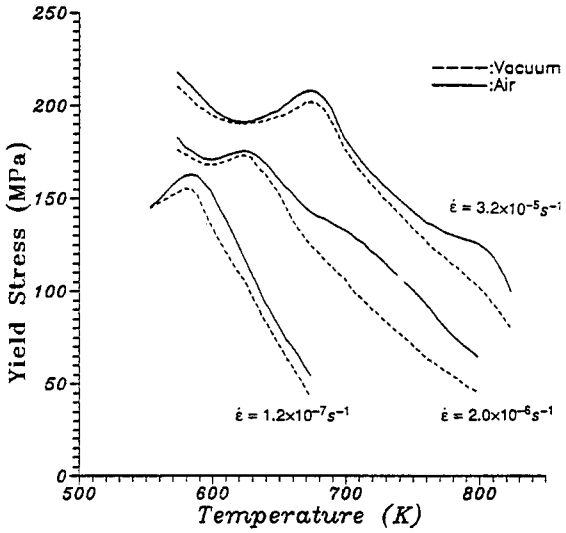


**Fig.4 Yield Stress of Zircaloy-4 vs. Temperature**

### 4.2 Solutes Responsible for Dynamic Strain Aging

From the above results, the Arrhenius plot of the strain rate versus the reciprocal of the yield stress peak temperature as shown in Fig.5 led to an activation energy of 196 KJ/mol for Zircaloy-4 tube. This value corresponds to the activation energy for oxygen diffusion in $\alpha$-zirconium (207 KJ/mol, by J.J. Kearns and J.N. *Chirigos*[21] and 213 KJ/mol, I.G. Ritchie and A. *Atrens*[22]), and in Zircaloy-2 (220 KJ/mol, R. Choubey and J.J. *Jonas*[23]). The activation energy obtained from elongation shift with the changes of strain rate was

205 KJ/mol by S.I.Hong et *al.*[13]. Therefore, it is clear that the yield stress peak is closely associated with the drag force due to oxygen atoms. It is reasonable to conclude that oxygen atoms are responsible for dynamic strain aging.

On the other hand, the yield stress peaks were observed at 723 K and 798 K only in air. With consideration, Fe could be responsible for strain aging peak observed in Zircaloy-2 and Zircaloy-4 at 725 *K*[20,24]. The yield stress peaks at 723 k and 798 K only in air might be due to Fe atoms.

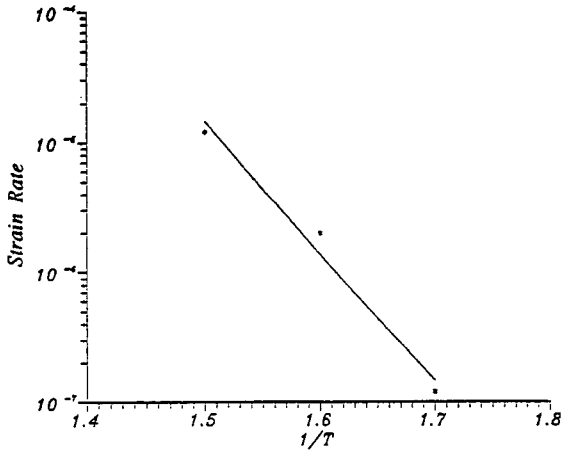


**Fig.5 ln ε vs. Reciprocal of Temperature**

### 4.3 Strain Rate Sensitivity

The strain rate sensitivity of Zircaloy-4, obtained from the yield stress data at two strain rates ($2.0\times10^{-6}s^{-1}$ and $3.2\times10^{-5}s^{-1}$), was plotted as a function of temperature in Fig.6. In general, the strain rate sensitivity tends to increase linearly with temperature in a number of metals. When it falls below this straight line, dynamic strain aging phenomena are also observed. Note the tendency for the strain rate sensitivity to be low in both the dynamic strain aging region near 623 K and near 723 K in air. But in vacuum, the strain rate sensitivity minimum near 723 K did not appeared.

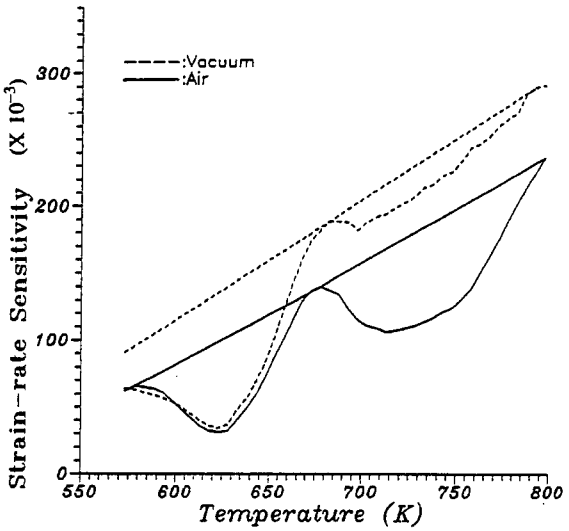


**Fig.6 Strain Rate Sensitivity of Zircaloy-4 vs. Temperature**

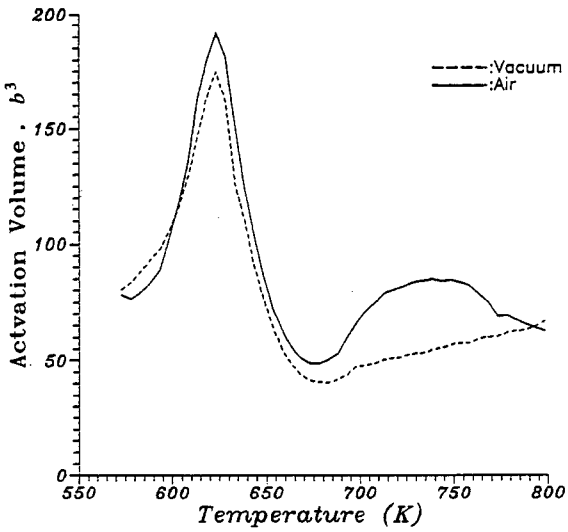


**Fig.7 Apparent Activation Volume of Zircaloy-4 vs. Temperature**

### 4.4 Apparent Activation Volume

The calculated apparent activation volume as a function of temperature varies between $40b^3$ and $190b^3$ in air and vacuum. As shown in Fig.8, in air, the large peak in apparent activation volume was observed at 623 K and the small peak observed at 723 K, but in vacuum the peak at 723 K was not appeared. These trends are identical

with the strain rate sensitivity as shown in Fig.6.

The temperature range where the peak in apparent activation volume occurs coincides with the strain rate sensitivity minimum temperature range obtained by above section (4.3), which means that the peak can be related to the dynamic strain aging.

### 4.5 Strengthening Due to Oxidation

The strength increases and the ductility decreases as the oxygen content increases. The strengthening is due to oxygen diffusion into the materials and stable oxide *layer*[25]. In other words, the slower strain rate, the more strengthening occurs. This effect is shown in Fig.8. The percentage increase of yield stress is obtained by comparing the yield stress in air with that in vacuum. Its equation is shown as follows,

$$P_i=\left(\frac{\sigma_{y}^{a}-\sigma_{y}^{v}}{\sigma_{y}^{v}}\right)\dot{\varepsilon}_{i}100 \quad \cdots\cdots (8)$$

These results, shown in Fig 8, are also identical with above estimation.

It is very important to obtain the yield stress increase in water. For this purpose, the oxidation rate in air and water must be considered in order to compare the weight gain($\Delta w$) of oxygen in air with that in water. The oxidation *rate*[26] is as follows,

$$\Delta w = k \cdot t \quad \cdots\cdots (9)$$

Although n value in Eq.(9) is varied with the environment, the oxygen partial pressure and the specimen geometry and preparation, this value is really equal to 1/2 (the parabolic rate law) in air and 1/3 (the cubic rate law) in water. If the yield stress increase in air ($\Delta\sigma_{y}^{a}=\sigma_{y}^{a}-\sigma_{y}^{v}$) is linearly proportional to the weight gain difference ($\delta w^{a}=\Delta w_a-\Delta w_v$), the yield stress increase in water ($\Delta\sigma_{y}^{w}=\sigma_{y}^{w}-\sigma_{y}^{v}$) can have the same relation with the weight gain difference ($\delta w^{w}=\Delta w_w-\Delta w_v$). These relations are as follws,

$$\Delta\sigma_{y}^{w}=\Delta_{y}^{a}\times\frac{\delta w^{w}}{\delta w^{a}} \quad \cdots\cdots (10)$$

Therefore,

$$\sigma_{y}^{w}=\sigma_{y}^{v}+\Delta\sigma_{y}^{w} \quad \cdots\cdots (11)$$

The results are given in Fig.9. In case of the two strain rates ($3.2\times10^{-5}s^{-1}$, $2.0\times10^{-6}s^{-1}$), the calculated yield stress in water ($\sigma_{y}^{w}$) is equal to $\sigma_{y}^{a}$ because of the short test time. However, at $\dot{\varepsilon}=1.2\times10^{-7}s^{-1}$, the yield stress in air test at 573, 598, 623, 648 and 673 K were 159.5, 154.5, 118.5, 82.5 and 54.5 MPa, respectively, and the calculated yield stress in water at these temperantures were 157.8, 151.4, 116.5, 80.9 and 52.5 MPa, respectively.

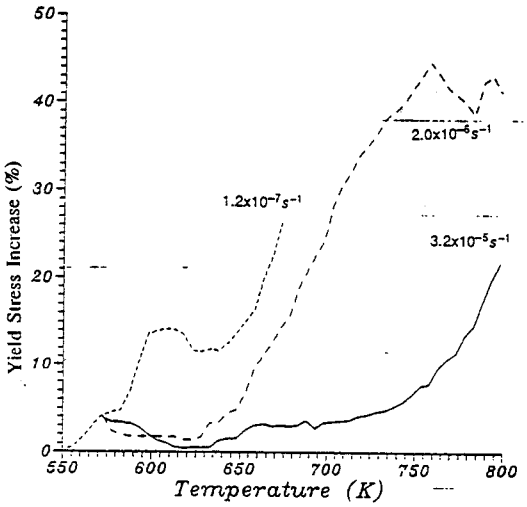


**Fig.8 Percentage Increase of Yield Stress of Zircaloy-4 vs. Temperature**

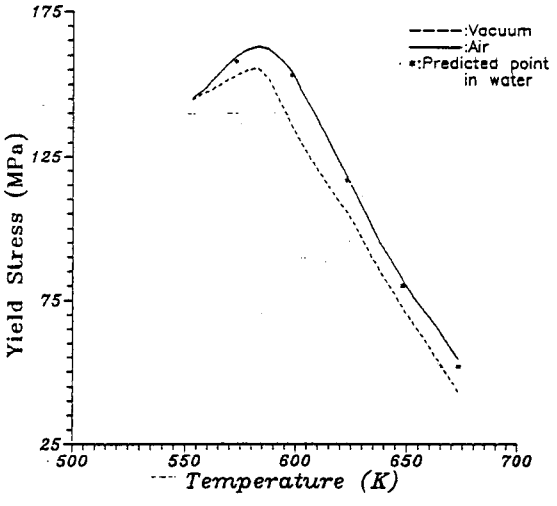


**Fig.9 The Predicted Yield Stress in Water**

## 5. Conclusions

(1) The yield stress peaks in air were observed at 576 K ($\dot{\varepsilon}=1.2\times10^{-7}s^{-1}$), 623 K & 73 K ($\dot{\varepsilon}=2.0\times10^{-6}s^{-1}$) and 673 K & 798 K ($\dot{\varepsilon}=3.2\times10^{-5}s^{-1}$), and these peaks in vacuum were observed at 576 K ($\dot{\varepsilon}=1.2\times10^{-7}s^{-1}$), 623 K ($\dot{\varepsilon}=2.0\times10^{-6}s^{-1}$) and 673 K ($\dot{\varepsilon}=3.2\times10^{-5}s^{-1}$). The yield stress peaks in air and vacuum are considered to be due to dynamic strain aging. These peaks observed at 576 K, 623 K and 673 K in air as well as vacuum should be due to the oxygen atoms, and those at 723 K and 798 K only in air might be due to the iron atoms.

(2) An activation energy for dynamic strain aging was 196 (kJ/mol). This value is in good agreement with the activation energy for oxygen diffusion in $\alpha$-zirconium and zircaloy-2. Therefore, oxygen atoms are responsible for dynamic strain aging which appeared at 573–673 K.

(3) In air, the strain rate sensitivity minimum as well as the activation volume peaks appeared at 623 K and 723 K, but in vacuum, such phenomena at 723 K did not appeared. The strain rate sensitivity minimum and the activation volume peaks could be explained in terms of the dynamic strain aging.

(4) Comparing the yield stress in air with that in vacuum ($5\times10^{-5}$ torr), the former was a little greater than the latter. And the slower strain rate, the greater percentage increase occurred.

(5) The calculated yield stress value in the water environment lies between experimental yield stress value in air and that in vacuum because the oxidation rate in air is faster than that in water at the same temperature. As a result, the calculated yield stresses in water ($\alpha_y^w$) at 573, 598, 623, 648 and 673 K were 157.8, 151.4, 116.5, 80.9 and 52.5 MPa, respectively.

## Reference

1. A.H. Cottrell, "Dislocation and Plastic Flow in Crystals", Oxford University Press, London, 1953.
2. V.Ramachandran and R.E. Reed-Hill, Met. Trans., 1, 2105(1970).
3. A.M. Garde, E. Aigeltinger, B.N. Woodruff and R.E. Reed-Hill, Met. Trans., 6A, 1183(1975).
4. A. Nadai and M.J. Manjoine, Trans. ASME, 63, A47–91(1941).
5. J.D. Baird and A. Jamieson, J. Iron Steel Inst., 204, 793–803(1966).
6. O.D. Sherby and A.K. Miller, "Development of the Materials Code, MATMOD", EPRI NP-567, 1977.
7. J.L. Derep, S. Ibranhim, R. Rouby and G. Fantozzi, Acta. Metall, 28, 607(1980).
8. P. Soo and G.T. Higgins, cta Metall., 16, 187(1968).
9. J.D. Lubahn, Trans. ASME, 44, 643–664(1952).
10. J.K. Yi and B.W. Lee, J. Korean Nucl. Soc., 19, 608–619(1987).
11. G.E. Diter, "Mechanical Metallurgy", 81, McGraw hill,(1986).
12. R.G. Reed-Hill, "Physical Metallurgy", 346–353, University Series in Basic Engineering,(1973).
13. S.I. Hong et al., J.Nucl. Mat., 116, 314–316(1984).
14. H. Conrad, J. Met., 16, 582(1964).
15. A.G. Evans and R.D. Rawlings, Phys. Stat Sol., 34, 9(1966).
16. M.J. Louton and J.J. Jonas, Can. Metall, 11 79(1979).
17. A.M. Grade, J. Nucl. Mat., 80, 195–206(1979)
18. W.R. Thorpe and I.O. Smith, J. Nucl. Mat., 78 49–57(1978).
19. S.I. Hong, W.S. Ryu and C.S. Rim, Nucl Mat., 120, 1–5(1984).
20. K.S. Rheem and W.K. Park, J.Kor. Nucl. Soc.

8, 19(1976).

21. J.J. Kearns and J.N. Chirigos, WAPD-TM-306, (1962).
22. I.G. Ritchie and A. Atrens, J. Nucl. Mat., 67, 254(1977).
23. R. Choubey and J.J. Jonas, Metal. Sci., 15, 30(1981).
24. K. Veevers, J.Nucl. Mat., 55, 109–110(1975).
25. H.M. Chung, A.M. Grade and T.F. Kassner, MSD "Light-Water-Reactor Safety Research Program : Quarterly Program Report", ANL-77-34.
26. B. Cox, "Oxidation of Zircoium and its Alloys", Advances in Corrosion Science and Technology, 4, 173(1970).